Mirco Andreotti, University of Ferrara
October 2002

New Form Factor Results with the Threshold at 120 MeV.

In `old` form factor analysis any cluster with $M_{cl} > 100$ MeV was split into two clusters by identifying a second cluster center. Recently it has been found (by Matteo) that this threshold has to be rise at 120 MeV in order to avoid the loose of about 7-8% of exclusive events $\psi' \to e^+e^-$. Since the form factor events are characterized by the same final state, we need to control the form factor results obtained with `new` threshold at 120 MeV.

Using `new` threshold could change the following things:

1. Number of form factor events.
2. Efficiencies of both preselection (ϵ_{pres}) and final selection (ϵ_{sel}), then also the overall efficiency (ϵ_{ana}).
3. Background contamination mainly from $J/\psi X$ events and events with at least one π^0 in the final state.
4. Values of the form factor.

We want to point out that `old` form factor analysis was applied to ewdst files, while `new` analysis has to be applied to mdst files, because ewdst files have been produced with the threshold at 100 MeV. In this way `new` ntuples have not preselected (with $\log_{10}(ew1 * ew2) > -1$), then we can use these also to calculate the efficiency of the preselection.

In the following sections we will show the results obtained with the threshold at 120 MeV. We will call `new` and `old` results obtained respectively with threshold at 120 MeV and 100 MeV.

1 Number of Form Factor Events

Applying the known form factor analysis in the same energy region we found 3 events more at h_c respect to `old` analysis. In Tab.1 `new` and `old` number of form factor events are reported:

Sample	$\sqrt{s}$ Interval (GeV)	Mean±Rms (GeV)	L (pb^{-1})	N
1	3.340-3.392	3.379±0.014	8.52	8
2	3.430-3.470	3.455±0.019	3.95	3
3	3.523-3.529	3.526±0.006	50.50	34 (31)
4	3.770-3.836	3.795±0.050	5.17	0
5	4.267-4.270	4.268±0.002	2.10	0

Table 1: Summary of data used for the form factor analysis. Between parenthesis `old` number of form factor events are reported.

As espected, `new` threshold increases the number of events of about 10% at h_c energy, while at the other energies the number of events remain unchanged.

Efficiency of the preselection

Using the same four samples used in `old` analysis [1] we calculated the `new` efficiency of the preselection. In Tab.2 `new` and `old` results are reported.

sample	ϵ_{pres}
1	0.963 ± 0.030 (0.969 ± 0.021)
2	0.940 ± 0.020 (0.960 ± 0.030)
3	0.947 ± 0.022 (0.966 ± 0.024)
4	0.950 ± 0.024 (0.967 ± 0.026)

Table 2: Efficiency of the preselection obtained from real samples of $\psi' \to e^+e^-$ events. Between parenthesis `old` values of the efficiency are reported.

Averaging the `new` values of Tab.2 we obtain the following preselection efficiency:

$$\epsilon_{pres}^{\texttt{new}} = 0.950 \pm 0.012(stat)^{+0.042}_{-0.030}(syst) \tag{1}$$

while `old` efficiency was:

$$\epsilon_{pres}^{\texttt{old}} = 0.966 \pm 0.013(stat)^{+0.027}_{-0.036}(syst) \tag{2}$$

2 Efficiency of final selection and of form factor analysis

As made in `old` analysis, subtracting the background at two different energies and using the same four samples [2] we obtain `new` eight values of the final selection efficiency reported in Tab.3 with also `old` values.

[1] See tab.6 at the end.
[2] See Tab.7 at the end.

Sample	ϵ_{sel}
1	$0.752^{+0.031}_{-0.030}$ $(0.716^{+0.030}_{-0.029})$
2	$0.688^{+0.030}_{-0.028}$ $(0.654^{+0.029}_{-0.028})$
3	$0.696^{+0.019}_{-0.017}$ $(0.666^{+0.019}_{-0.017})$
4	$0.691^{+0.025}_{-0.024}$ $(0.682^{+0.025}_{-0.024})$

(a)

Sample	ϵ_{sel}
1	$0.751^{+0.030}_{-0.030}$ $(0.716^{+0.030}_{-0.029})$
2	$0.686^{+0.029}_{-0.028}$ $(0.653^{+0.029}_{-0.028})$
3	$0.695^{+0.018}_{-0.017}$ $(0.665^{+0.018}_{-0.017})$
4	$0.690^{+0.024}_{-0.024}$ $(0.682^{+0.025}_{-0.024})$

(b)

Table 3: Efficiency of final selection: `(a)` background at 3666 MeV, `(b)` background at 3704 MeV. Between parenthesis `old` values of the efficiency are reported.

Averaging the values in Tab.3 the final selection efficiency is:

$$\epsilon_{sel}^{\texttt{new}} = 0.706 \pm 0.009(stat)^{+0.046}_{-0.020}(syst) \tag{3}$$

while `old` value was:

$$\epsilon_{sel}^{\texttt{old}} = 0.679 \pm 0.009(stat)^{+0.037}_{-0.026}(syst) \tag{4}$$

The efficiency of the form factor analysis is $\epsilon_{ana} = \epsilon_{trig}^{data} \cdot \epsilon_{pres}^{data} \cdot \epsilon_{sel}^{data}$:

$$\epsilon_{ana}^{\texttt{new}} = 0.604 \pm 0.017(stat)^{+0.047}_{-0.025}(syst) \tag{5}$$

`old` value was:

$$\epsilon_{ana}^{\texttt{old}} = 0.590 \pm 0.017(stat)^{+0.036}_{-0.032}(syst) \tag{6}$$

`New` and `old` values are comparable within the errors.

Fig.1 shows `new` invariant mass distribution for candidate electron after preliminary selection `(a)` and after final selection `(b)` at the ψ' formation energy. The cross-hatched areas in both histograms correspond to the background contamination in these samples, extracted applying the same analysis to the data taken off resonance at $\sqrt{s} = 3.7$ GeV. Horizontal lines correspond to the decay $\psi' \to J/\psi X$ selected requiring $Prb(J/\psi X) > 1\%$ and $Prb(e^+e^-) < 10\%$ (with a `new` efficiency of $\sim 87\%$). It can be seen that the background contamination from J/ψ-inclusive decay is very small.

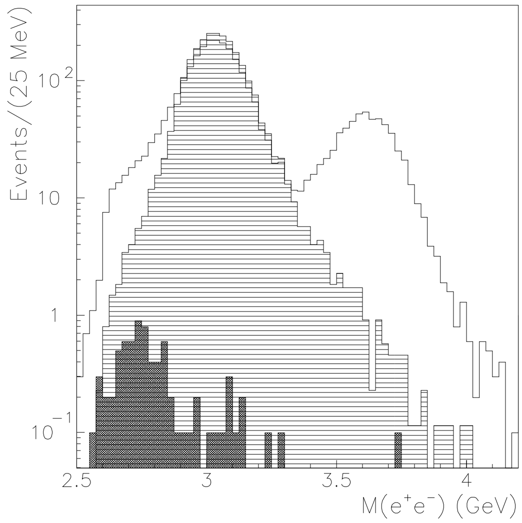

(a)

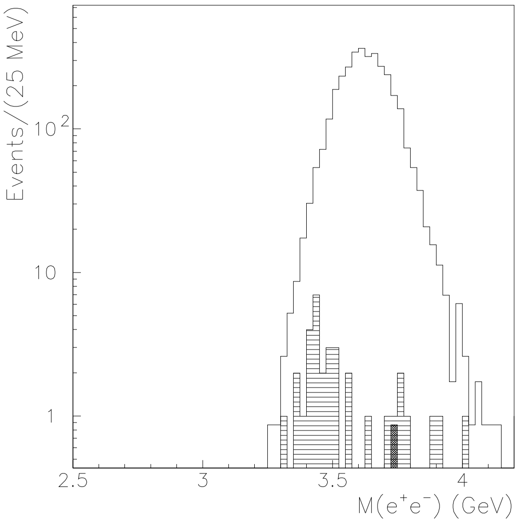

(b)

Figure 1: Invariant mass distribution for candidate electrons after preliminary selection `(a)` and after final selection `(b)`: at ψ' energy (white) and at $\sqrt{s} = 3.7$ GeV (cross-hatched); horizontal lines correspond to J/ψ-inclusive subsample at ψ' energy. (The number of events has been rescaled by luminosity).

3 Studies of background reaction.

`New` threshold could change the background contamination from which final states that contain e^+e^- and/or π^0. Then we have to recalculate the background contamination from $J/\psi X$ events and from photon conversions and π^0 Dalitz decay. The hadronic final states should not be sensitive to a change of threshold.

3.1 Inclusive J/ψ

At the two energies out of the χ_0 peak the source of inclusive contamination is the decay $\chi_0 \to J/\psi\gamma$. We select form factor events at χ_0 peak and we consider these as due to $\chi_0 \to J/\psi\gamma$ decay, then rescaling with Breit-Wigner formula we found the espected background cross section out of the χ_0 peak [3].
Appling form factor selection at all energies of the χ_0 we find the same number of events found with `old` threshold, then we will use the same background cross section evaluated in `old` analysis.

At the energy of the h_c we remeasure the fraction α[4] which now is:

$$\alpha^{\mathtt{new}} = 4 \times 10^{-3} \tag{7}$$

while the `old` value was:

$$\alpha^{\mathtt{old}} = 3 \times 10^{-3} \tag{8}$$

[3] See my memo for more details.
[4] See my memo for more details.

3.2 Photon conversions and π^0 Dalitz decay

In order to evaluate the contamination from photon conversions and π^0 Dalitz decay we need to measure η and ω[5].
To measure η in `old` analysis we used a sample of $\overline{p}p \to \pi^0\pi^0$ events, where the π^0 has been selected requiring $|M_{\gamma\gamma} - M_{\pi^0}| < 35$ MeV. If now we use the `new` threshold we could lose $\pi^0\pi^0$ events, then η we will use `old` value of η. While ω has to be measured with `new` threshold and we obtain that `new` and `old` value are the same ($\omega < 10^{-2}$).

3.3 Total background cross section

Using `new` value of α we calculated the expexted background cross sections reported in Tab.4, also `old` values are reported between parenthesis.

s (GeV^2)	$\sigma_{J/\psi X}$ (pb)	σ_p (pb)	σ_h (pb)	σ_B (pb)
11.42	3.0×10^{-2}	3.1×10^{-3}	4.3×10^{-3}	3.7×10^{-2}
11.93	2.3×10^{-2}	2.0×10^{-3}	3.6×10^{-3}	2.9×10^{-2}
12.43	2.0×10^{-2} (1.5×10^{-2})	1.7×10^{-3}	2.9×10^{-3}	2.5×10^{-2} (2.0×10^{-2})
14.40	$< 2.0 \times 10^{-2}$ (1.5×10^{-2})	$< 0.9 \times 10^{-3}$	$< 0.7 \times 10^{-3}$	$< 2.2 \times 10^{-2}$ (1.7×10^{-2})
18.22	$< 2.0 \times 10^{-2}$ (1.5×10^{-2})	$< 0.9 \times 10^{-3}$	$< 0.7 \times 10^{-3}$	$< 2.2 \times 10^{-2}$ (1.7×10^{-2})

Table 4: Expected background cross section from inclusive $J/\psi X$ reaction ($\sigma_{J/\psi X}$), photon conversions (σ_p) and from $\pi^+\pi^-$ final state (σ_h). σ_B is the total background cross section. Between parenthesis `old` values are reported.

Again the background contamination is negligible.

4 Measurements of the magnetic form factor of the proton

In Fig.2 we compare `new` magnetic form factors with `old` values.
Tab.3 shows `new` and `old` results.
Fig.3 shows `new` values of the magnetic form factor of the proton.

[5] See my memo

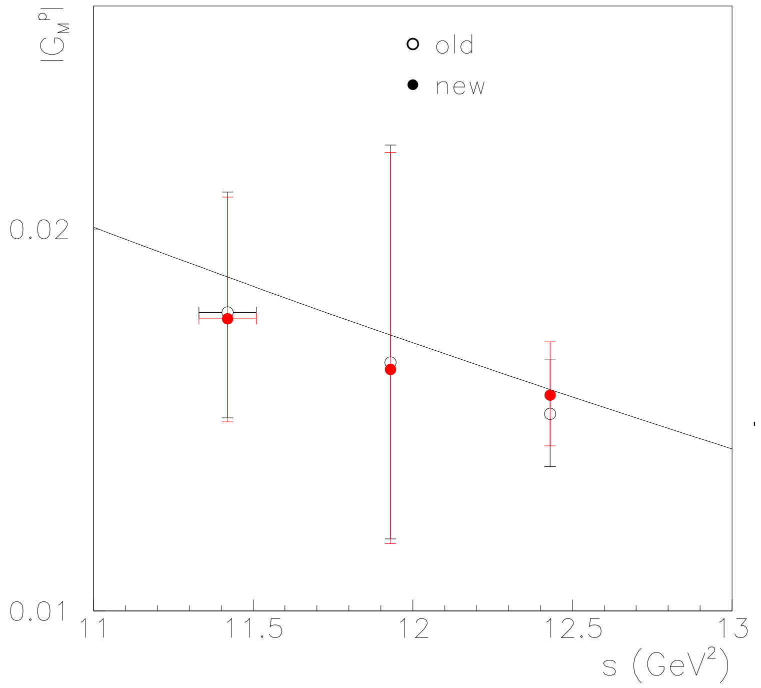

Figure 2: Comparison between `new` and `old` magnetic form factor.

s (GeV^2)	L (pb^{-1})	N	σ_{acc} (pb)	$\|\cos\theta^*\|_{max}$	$10^2 \times \|G_M\|$ (a)	(b)
11.42±0.09	8.52	8	$1.56^{+0.77+0.12}_{-0.54-0.06}$ ($1.59^{+0.79+0.10}_{-0.55-0.09}$)	0.568	$1.70^{+0.42+0.07}_{-0.29-0.04}$ ($1.72^{+0.42+0.05}_{-0.30-0.05}$)	$1.90^{+0.47+0.07}_{-0.33-0.04}$ ($1.92^{+0.47+0.06}_{-0.33-0.05}$)
11.93±0.13	3.95	3	$1.26^{+1.22+0.10}_{-0.68-0.05}$ ($1.29^{+1.25+0.08}_{-0.70-0.07}$)	0.585	$1.55^{+0.75+0.06}_{-0.42-0.03}$ ($1.57^{+0.76+0.05}_{-0.43-0.04}$)	$1.72^{+0.84+0.07}_{-0.47-0.04}$ ($1.74^{+0.85+0.05}_{-0.47-0.05}$)
12.43±0.01	50.50	34 (31)	$1.11^{+0.23+0.09}_{-0.19-0.05}$ ($1.04^{+0.22+0.06}_{-0.19-0.06}$)	0.601	$1.48^{+0.15+0.05}_{-0.13-0.03}$ ($1.43^{+0.15+0.04}_{-0.13-0.04}$)	$1.63^{+0.17+0.06}_{-0.14-0.03}$ ($1.58^{+0.17+0.05}_{-0.14-0.04}$)
14.40±0.19	5.17	0	< 0.80 (< 0.82)	0.603	< 1.38 (< 1.40)	< 1.51 (< 1.53)
18.22±0.01	2.10	0	< 1.98 (< 2.03)	0.512	< 2.77 (< 2.81)	< 2.99 (< 3.03)

Table 5: Summary of the results of the form factor analysis. For each energy regio the integradted luminosity L, the selected number of events N, the cross section $\sigma_{acc} = N/(\epsilon \cdot L)$ are reported. $|\cos\theta^*|_{max}$ is the maximum value of $|\cos\theta^*|$ where θ^* is the scattering angle in c.m.; (a) $|G_M|$ calculated in the hypothesis $|G_E| = |G_M|$; (b) $|G_M|$ calculated in the approximation of negligible electric contribution. Between parenthesis we report old results.

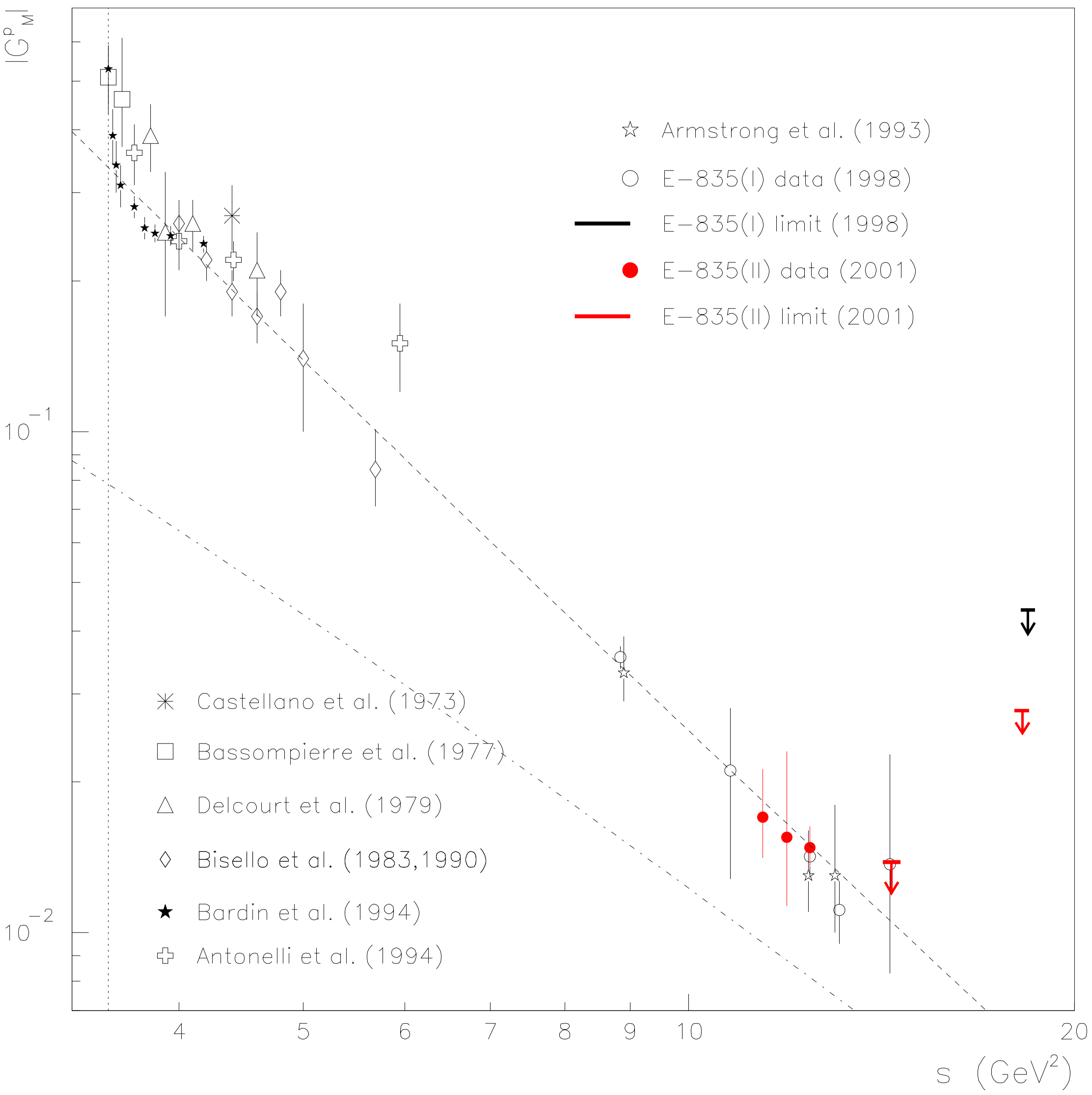

Figure 3: All existing values of the magnetic form factor in timelike region obtained with the hypothesis $|G_M| = |G_E|$. Upper limits are evaluated at 90% CL. We have also shown the asymptotic behavior in timelike region (solid line), dipole behavior in spacelike region (line dash-point) and the threshold value of timelike region (dotted line): $s = 4m_p^2$.

5 Samples used for the efficiencies calculation

sample	mdst file	run	E_{cm}	$\int Ldt$ (pb^{-1})
1	00-01-27	5006,5009	ψ' peak	2.40
		5012-5038		
	00-01-31	5076-5084		
2	00-04-30	5571-5574	ψ' peak	4.95
	00-06-14	5818-5834		
		5837		
	00-06-16	5840-5842		
	00-08-26	7143-7148		
3	00-10-09	7248	ψ' peak + bckg	4.52
		7250-7252		
	00-10-15	7254-7259		
	00-11-06	7269-7271		
4	00-11-07	7273-7278	ψ' peak	1.94

Table 6: Samples of mdst data used in the calculation of preselection efficiency.

Sample	run	E_{CM} (MeV)	$\int Ldt$ (pb^{-1})
1	$5006 \div 5084$	3686	1.756
2	$5571 \div 5574$		
	$5818 \div 5842$	3686	2.380
3	$7144 \div 7259$	3686	5.944
4	$7273 \div 7278$	3686	2.401
bkg	$7280 \div 7283$	3666	0.779
bkg	$7269 \div 7271$	3704	1.153

Table 7: Four samples at the ψ' peak and two background above and below the peak.